PROCEEDINGS OF SCIENCE

White Dwarfs and metallicity: lights and shadows

J.Isern[a,b,c,*]

[a] *Institute for Space Science (ICE,CSIC),*
Campus UAB, Cerdanyola del Vallès, Catalonia, Spain
[b] *Institut d'Estudis Espacials de Catalunya (IEEC),*
PMT-Campus Baix Llobregat (UPC), 08860 Castelldefels (Barcelona), Catalonia, Spain
[c] *Observatori Fabra, Sec.1a, Reial Acadèmia de Ciències i Arts de Barcelona (RACAB),*
Rambla dels Estudis 115, 08002 Barcelona, Catalonia, Spain

E-mail: isern@ice.csic.es, isern@ieec.cat

White dwarfs are the final remnants of low and intermediate mass stars and their evolution is essentially a long lasting gravothermal process of cooling that allows them to be used for reconstructing or at least for constraining the evolution of several Galactic populations of stars since it is possible to relate their cooling age with their luminosity. At present, the number of white dwarfs with reasonably good parallaxes and photometric data is 300,000 thanks to the Gaia mission. These data together with the spectroscopic information obtained by different surveys have shown the existence of structures in the HR-domain of white dwarfs and have provided luminosity functions of unprecedented precision that open new perspectives about the evolution of white dwarfs. One of them is crystallization. This process releases energy via latent heat and through the sedimentation of heavier chemical species by a change of solubility during the transition liquid-solid and consequently it slows down the cooling evolution. This effect raises a new problem, the dependence on the initial metallicity, an aspect that cannot be longer neglected and that it is hard to include since it is impossible to estimate the original metallicity of the parent star of isolated white dwarfs. One possible way to solve or to palliate this problem is to obtain the luminosity function of white dwarfs that are members of non-interacting binaries.

The Golden Age of Cataclysmic Variables and Related Objects - VI (GOLDEN2023)
4-9 September 2023
Palermo - (Mondello), Italy

*Speaker

PoS(GOLDEN2023)009

1. Introduction

White dwarf stars have a relatively simple structure. Those in the range of $0.4 \lesssim M/M_\odot \lesssim 1.1$ have a core made of a mixture of ^{12}C and ^{16}O plus some impurities being ^{22}Ne and ^{56}Fe the must abundant. This core, which is electron degenerate, is surrounded by two layers, the inner one being made of He and the outer one, which is absent in $\sim 20-30\%$ of stars, made of H. Their masses are $M_{He} \simeq 10^{-2}\, M_\odot$ and $M_H \lesssim 10^{-4}\, M_\odot$, respectively. Because of the degeneracy of electrons, white dwarfs cannot obtain energy from nuclear reactions and their evolution can be viewed as that of a degenerate core containing the bulk of mass and acting as an energy reservoir, surrounded by a semi-degenerate/non-degenerate envelope that controls the flux of energy from the interior to the free space. This simple structure and their long cooling times make them the ideal stellar object to characterize the properties of Galactic substructures, trace the evolution of the Galaxy and test new ideas in Physics. Furthermore, they are responsible of many energetic events like supernovae, novae, cataclysmic variables, and so on.

The age of stars is a fundamental parameter hard to obtain. In the case of non-degenerate stars several methods (chromospheric activity, isochrones, asteroseismological and so on) have been used [90]. In general the associate precision is of the order of $\sim 20\%$, although asteroseismological methods can be highly accurate. Since the evolution of white dwarfs is a simple gravothermal process, it is possible to build a relationship between its luminosity and its cooling time, often called photometric age, with an estimated accuracy of the order of 5%.

Unfortunately the situation is not so optimistic. The first problem is that the total age of a white dwarf is the photometric age plus the age of the progenitor, being the last one strongly dependent on the progenitor mass. As far as the mass of the progenitor is known via the poorly determined initial final mass relationship (IFMR), the uncertainty can be very large, specially in the case of low mass white dwarfs, although not in the case of massive white dwarfs, $0.9 \lesssim M_{WD} \lesssim 1.2$ M$_\odot$, for which the lifetime of the progenitor can be often neglected as compared with the cooling time [44]. The second problem is that the photometric time depends on the initial metallicity, which is not known in the case of isolated white dwarfs[1].

2. The photometric age

The main source of energy of white dwarfs is the gravothermal readjustment of its structure, complemented with the latent heat and sedimentation associated to crystallization, as well as with the gravitational diffusion of heavy chemical species like ^{22}Ne. The sinks of energy are thermal neutrinos, that freely escape, and photons that diffuse through the envelope. A detailed discussion can be found in [1, 19, 35, 48, 55, 82].

[1]Parts of this contribution were also presented during the workshops 22nd European Workshop on White Dwarfs (EUROWD22), S.Lauer, T Rauch, August 15-19, 2022, Tubingen (Germany), and Stellar evolution along the HR diagram (MW-Gaia Workshop), G. Clementini and M. Marconi, September 20-23, 2022, Naples, Italy, both unpublished. In the second case the corresponding viewgraphs can be found at https://drive.google.com/drive/folders/1O56LZpqy0EcgMvGpN3780fwS4MEY4U30?usp=sharing.

The evolution of their luminosity can be described by:

$$L + L_\nu = -\int_{M_{WD}} c_V \frac{dT}{dt} dm - \int_{M_{WD}} T\left(\frac{\partial P}{\partial T}\right)_{V,x} \frac{dV}{dt} dm + \int_{M_{WD}} \left[g_s + (l_s + e_s)\,\dot{m}_s \pm (\dot{\varepsilon}_e)\right]\, dm \quad (1)$$

where the gravothermal readjustment of the structure is represented by the first two terms of the r.h.s. of Equation 1, the gravitational induced diffusion of heavy species like ^{22}Ne by g_s, the latent heat and sedimentation associated to crystallization by $l_s + e_s$ times the crystallization rate $\dot{m}_s$, and any other exotic and hypothetical source or sink of energy by $(\dot{\varepsilon}_e)$. The l.h.s. of Equation 1 contains the sinks of energy, photons and neutrinos. If this equation is complemented with a relationship connecting the temperature of the core with the luminosity of the star[2] it allows to obtain the so called *photometric age* of the white dwarf or equivalently, the time that the white dwarf has been cooling, and use white dwarfs as an efficient forensic tool to study the temporal evolution of the Galaxy.

3. Influence of the initial conditions

One of the main problems is the determination of the initial conditions of the evolution of white dwarfs, which are strongly dependent on the amount of residual hydrogen left at the end of the Asymptotic Giant Branch (AGB) stage. If it is large enough, $M_H \gtrsim 10^{-4}$, hydrogen burning via pp-reactions never stops and it can be even dominant at low luminosities. Fortunately, asteroseismological observations seem to constrain the mass of hydrogen well below such a critical value.

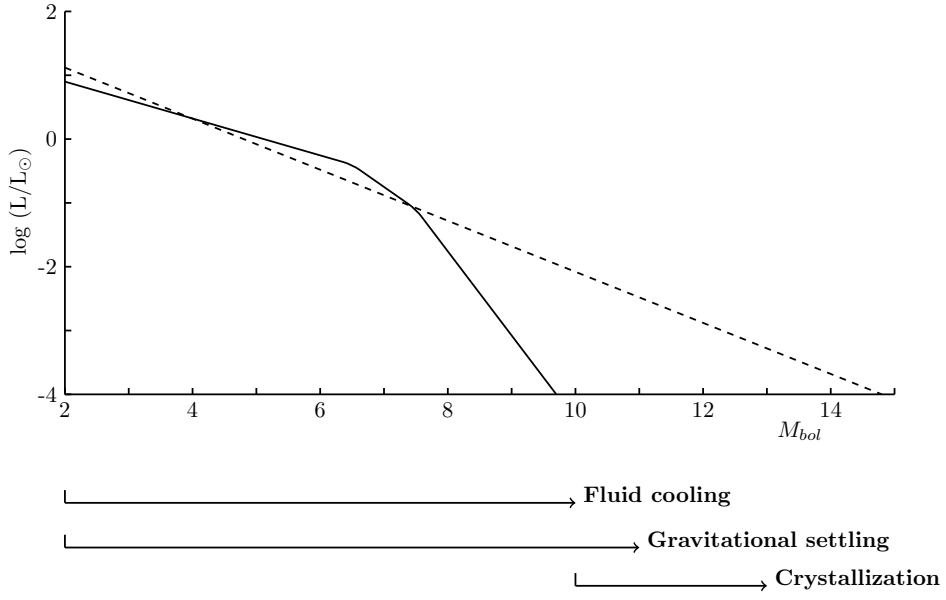

Figure 1: Photon and neutrino luminosities (dashed and continuous lines) versus the magnitude

[2]Typically $L \propto T_c^\alpha$ with $\alpha \approx 2.5 - 2.7$, although it depends on the nature of the envelope.

At very early times, the main contributor to the luminosity of the nascent white dwarf is hydrogen burning via CNO cycle and is during this epoch that the final thickness of the hydrogen layer is configured. This stage is very short, $\sim 10^4$ yr, nuclear reactions cease abruptly, and the luminosity drops from $\log(L/L_\odot) \approx 4$ to $\log(L/L_\odot) \approx 1-2$ [1]. From this moment neutrino emission becomes dominant, Figure 1, and forces the different thermal structures to converge to a unique one at $\log(L/L_\odot) \approx -1.5$ [19]. The comparison between the evolution times obtained with the LPCODE and the BaSTI codes using exactly the same inputs differ at this epoch by an 8% as a consequence of the different converged models at the beginning of the cooling sequence [77].

After $10^7 - 10^8$ yr, depending on the mass of the star, neutrino emission rapidly drops since $L_\nu \propto T_C^7$ at this stage and photon losses become dominant once more (Fig. 1). At this epoch photon luminosity is controlled by a thick non-degenerate layer with an opacity dominated by hydrogen, if present, and helium that is weakly dependent of the metal content [1, 19, 35]. At the same time, the core of the white dwarf behaves like a fluid which can be described as a Coulomb plasma not very strongly coupled, $\Gamma < 178$ [50, 68, 87][3]. At this stage a key ingredient is the electron conductivity in the frontier between moderate and strong degeneracy. If the Blouin et al. [8] is used instead of that of Cassisi et al. [16], models predict longer cooling times at high luminosities and shorter cooling times at low luminosities [16, 81].

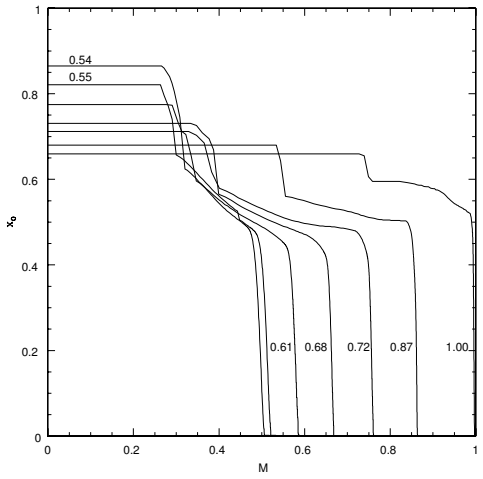

Figure 2: Oxygen distribution in the interior of white dwarfs with different masses [79].

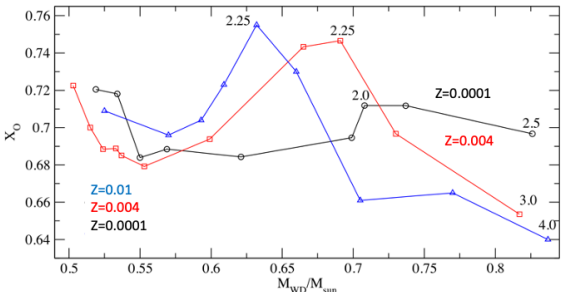

Figure 3: Central oxygen abundances versus de mass of the white dwarf for three metallicities [73]. Numbers give the mass of several progenitors.

The dependence of the specific heat on the chemical composition introduces an important source of uncertainty in the cooling rate of white dwarfs. The abundance of oxygen in the center is larger than in the outer layers and this tendency increases when the mass decreases (Fig. 2). This behaviour is controlled by the rate of the reaction $^{12}C(\alpha,\gamma)^{16}O$ and by the treatment given to semiconvection and overshooting [78, 79] which are both uncertain and depend on the metallicity as it can be seen in Figure 3. Fortunately, asteroseismological techniques have started to provide

[3]The Coulomb parameter $\Gamma = Z^2e^2/ak_BT$, where $a = [3/(4\pi n_i)]^{1/3}$ is the ion-sphere radius, n_i is the ion number density and k_B is the Boltzmann constant, compares the energy of the Coulomb interaction with the thermal energy. In the case of one component plasma the transition liquid-solid occurs for $\Gamma \simeq 178$

direct information about the internal structure and have confirmed the stratified nature of the C/O core [20, 31, 74].

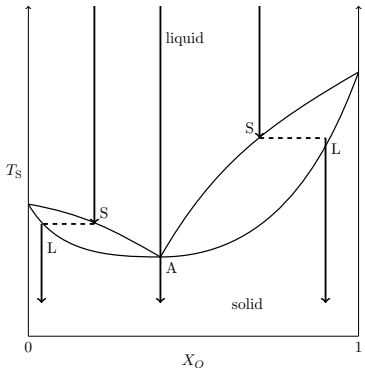

Figure 4: Carbon-oxygen phase diagram. The cooling tracks are represented by arrows. The liquid solid coexistence is represented by a dashed line. The azeotropic point is represented by A

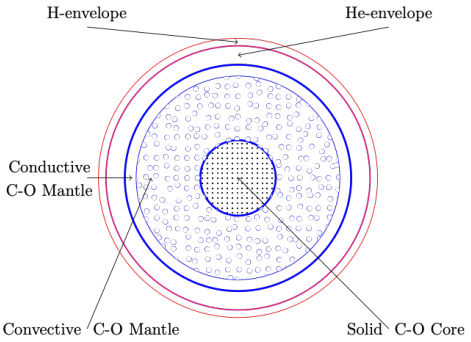

Figure 5: Structure of a crystallizing CO white dwarf star.

When the temperature is low enough, the plasma experiences a phase transition and crystallizes into a classical body-centered cubic crystal (bcc), the detailed structure being rather uncertain since the free energy of the different Coulomb crystals is very similar at low temperatures. Solidification introduces two additional sources of energy in the cooling process, latent heat and gravitational sedimentation. The contribution of the latent heat was early recognized [88, 96]. It is of the order of $k_{\rm B}T_{\rm s}$ per nuclei, where $k_{\rm B}$ is the Boltzmann constant and $T_{\rm s}$ is the temperature of solidification. The total energy released is not very high but since it happens at relatively low luminosities the cooling delay is not negligible.

During the process of crystallization of a C/O mixture the chemical composition of the solid and liquid plasmas that are in equilibrium are not necessarily equal [84]. The first phase diagram of the two dominant chemical species, ^{12}C and ^{16}O, was obtained by Stevenson [91] who found a complete separation of both species at the solid phase. These calculations were improved by several authors [36, 65] who found an azeotropic behaviour (Figure 4). This phase diagram was reexamined 20 years later [7, 34, 60] confirming the azeotropic behaviour of the mixture upon crystallization and the azeotropic abundance of oxygen being $x_O \approx 0.2$ (number fraction). Given the expected relative abundances of carbon and oxygen, the solid that forms contains more oxygen, is denser than the liquid, and settles down, while the liquid, which contains an excess of carbon, is redistributed by Rayleigh-Taylor instabilities. Figure 5 displays the resulting structure which remembers that of the Earth, a solid inner core surrounded by a fluid outer core[4]. The result is an enrichment of oxygen in the central layers and a depletion in the outer ones, with the subsequent release of gravitational

[4]Given the similitude, it has been suggested that this convective structure could generate a dynamo able to create a magnetic field [49], or to facilitate the emergence of a fossil field in the case of magnetic white dwarfs (https://indico.ph.tum.de/event/7409/contributions/8008/attachments/5531/7273/Isern_Slides.pdf).

energy [7, 33, 39, 47, 48, 71, 76, 87]. The energy release is smaller if oxygen is more abundant in the center and, obviously, the efficiency of the process depends on the detailed chemical structure, decreasing if the abundance of oxygen is already higher in the central regions of the star (Figures 2 and 3).

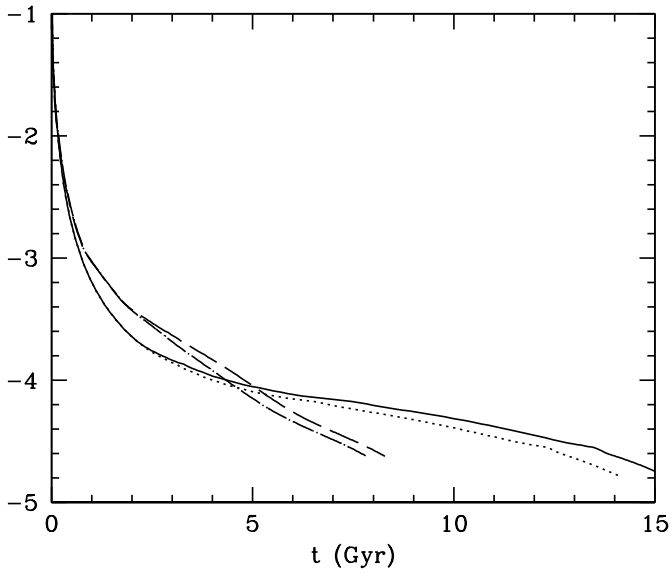

Figure 6: Luminosity versus time for a 0.6 solar mass white dwarf. Solid line: DA model. Dotted line: Same model but ignoring phase separation. Dashed and dotted-dashed lines represent, respectively, a non-DA model with and without separation [42].

The cooling time and the delays introduced by these effects depend on the thickness of the H and He envelope layers since they control the outflow of energy, i.e. $\Delta t \approx \Delta E/L$. This property is a matter of debate and it is not clear if the mass of these layers is the result of a global mechanism or the result of a stochastic process that depends on the individual stellar properties, specially during the AGB phase. Figure 6 displays the influence of the C/O sedimentation together with the presence or absence of a thick hydrogen layer of 10^{-4} $M_\odot$. Models with layers of different mass can be found in [69, 92]

3.1 Lifetime of the progenitor

The time necessary to produce a white dwarf depends not only on the mass of the progenitor, but also significantly on the metallicity. Figure 7 displays the ages obtained from two independent calculations. As it can be seen, low metallicity stars have systematically smaller lifetimes than those with solar metallicity. In the case of 1 $M_\odot$, for instance, the lifetime difference can be as large as a factor 2. Since it is not possible to estimate the initial metal content in the case of isolated white dwarfs, the age of the progenitor, specially if it is a low mass white dswarf, will be affected by an intrinsic uncertainty which can be overcome or partially palliated if the white dwarf is a member of a cluster, a wide binary, or the metallicity distribution of the population at which it belongs is known.

M_{Ms}	T_{ps}(Ga)			
	Z=0.0001	Z=0.001	Z=0.01	Z=0.02
0.80	12.742			
0.85	10.327	13.322		
0.90	8.421			
0.95	6.998		13.350	15.160
1.00	5.871	7.442	11.117	12.512
1.50	1.593	1.897	2.700	
2.00	0.752	0.947	1.211	1.286
2.50	0.423		0.742	
3.00	0.274	0.326	0.443	

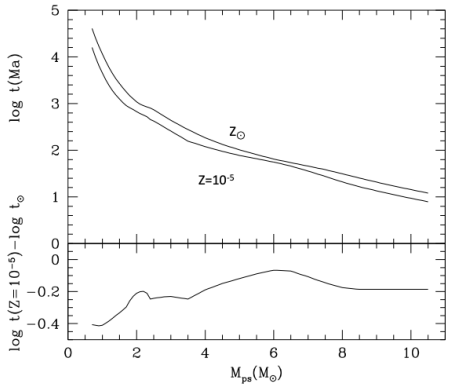

Figure 7: Lifetime of the progenitor versus the main sequence mass for different metallicities independently obtained by Romero et al. [73] (left, in giga-annum) and Pietrinferni et al. [67] (right,in mega-annum). The bottom of the figure displays the relative differences between the $Z = 10^{-5}$ and the $Z = Z_{\odot}$ cases.

3.2 Initial-final mass relationship

The mass of the white dwarf progenitors lies in the range $M/M_{\odot} \lesssim 8-10$, and the relationship that connects this mass with that of white dwarfs is known as the initial-final mass relationship (IFMR). The evolution during the main sequence is reasonably well known as well as that of white dwarfs, but the evolution during the RGB and specially during the AGB phases remains elusive and at present it is not possible to predict how much mass is lost during these stages. The first attempt to empirically map this function was due to Weidemann in 1977 [97] and since then its has been noticeably improved using semiempirical arguments [3, 4, 17, 18, 23, 24, 52, 72, 80, 98]. One method consists on obtaining the age of a coeval non-degenerate star in the case of white dwarfs that are members of a cluster or a wide binary and, after subtracting the cooling time of the white dwarf, the mass of the progenitor is obtained via an age-mass relationship. Another possibility is provided by the comparison of the white mass distributions obtained from synthetic populations and the observed one in a volume limited sample.

There are still several aspects not well known like the dependence of the total mass expelled during the RGB/AGB phases on the metallicity, magnetic field and angular momentum, or the incidence of mergers. When all these aspects are taken into account, the IFMR broadens noticeably introducing important uncertainties in the determination of the total age of the white dwarf and, consequently, on the evolution of galactic populations. This is clearly seen in the analysis of the influence of the metallicity in the mass distribution of the 40 pc sample [18], and on the theoretical[5] IFMRs displayed in Fig. 8 [67, 73]. There are several points in this figure that merit a comment:

1. Low metallicity stars produce white dwarfs with larger mass. The difference in mass can be as large as 40%. This means that the white dwarf mass distribution of a multiple-metallicity population will be different form one containing a single-metallicity one. Since the mass of the progenitor is infered from the mass of the white dwarf and, in the case of isolated stars, the metallicity is not known, the uncertinty in the parent star mass and age can be very large.

[5]Several groups have computed this relationship (BaSTI, LaPlata, Montreal,Padua, Postdam...).They differ in several aspects, specially those concerning the thermally pulsing asymptotic giant branch (TP-AGB) [99].

2. The mass of white dwarfs with masses $\lesssim 1.5 - 2$ $M_\odot$ are not strongly dependent of the metallicity but its distribution is relatively flat, i.e. $dm_{WD}/dM_{ps} \approx 0$, and can oscillate (this result can also be seen in [59, 99]. As before, this means that low mass white dwarfs around the peak can be produced by a relatively wide range of low mass progenitors. Taking into account the strong dependence of the lifetime with the mass this can introduce severe uncertainties.

M_{MS}	M_{WD}			
	Z=0.0001	Z=0.001	Z=0.01	Z=0.02
0.80	0.519			
0.85	0.534	0.505		
0.90	0.550			
0.95	0.561		0.493	0.488
1.00	0.569	0.553	0.525	0.511
1.50	0.669	0.627	0.570	
2.00	0.737	0.693	0.609	0.591
2.50	0.826		0.660	
3.00	0.875	0.864	0.705	

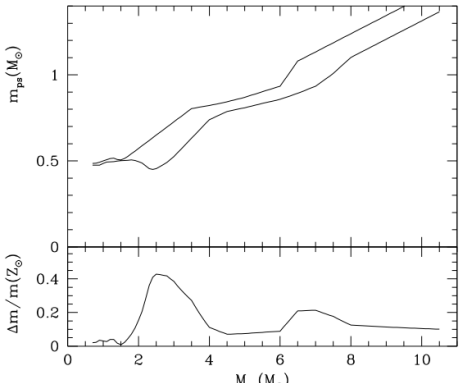

Figure 8: Mass of the white dwarf versus the progenitor mass for different metallicities independently obtained by Romero et al. [73] (left) and Pietrinferni et al. [67] (right). The bottom of the figure displays the relative differences between the $Z = 10^{-5}$ and the $Z = Z_\odot$ cases.

4. Energy release by impurities

Isotopes with small Z/A ratios, like ^{22}Ne, can play an important role during the cooling of white dwarfs. This isotope is the result of the α-burning of the ^{14}N left at the end of the H-burning stage and its abundance is of the order of the sum of C, N and O initial abundances of the parent star i.e. $X(^{22}\mathrm{Ne}) \approx 0.02$ in the case of solar metallicities. Because of this neutron excess and the high sensitivity of degenerate stellar structures to the electron number profile, Y_e, its migration towards the central regions of the white dwarf can represent an important source of gravitational energy despite its low abundance [38, 47]. A similar role, although less important because of its abundance, can be played by ^{56}Fe. As it is obvious, the incidence of these impurities depends essentially on the initial metallicity of the parent stars.

During the fluid phase a mixture of C/O/Ne remains mixed [65] and the only mechanism able to induce a migration of ^{22}Ne towards the central regions is through gravitational diffusion. The corresponding local diffusion times cale was estimated to be [11],

$$\tau\ (\mathrm{Gyr}) = 2.24 T_8^{-1/3} m^{-1} \rho_8^{11/18} \left[Z \left| \frac{\langle A \rangle}{\langle Z \rangle} - \frac{A}{Z} \right| \right]^{-1} \tag{2}$$

where T_8 and ρ_8 are the temperature and density, respectively, in units of 10^8, which suggests that diffusion is efficient only in the envelope and in hot interiors, $T_8 \geq 1$. However, since this early epoch lasts for a short time as a consequence of the neutrino emission, it was concluded that

^{22}Ne was not able to appreciably migrate before crystallization unless the diffusion coefficient was increased by an order of magnitude. A re-analysis with improved physics indicated that, effectively, this mechanism is not efficient in low mass white dwarfs, the majority, but it could work in massive ones, $M \gtrsim 1.0$ M$_\odot$ [6, 22]. Self-consistent calculations assuming that the diffusion within the crystal is negligible have shown that in the case of a 0.6 M$_\odot$ star the delay is negligible, while in the case of a 1.06 M$_\odot$ is ~ 3.2 Gyr and ~ 0.6 Gyr for a pure carbon and a pure oxygen white dwarf cases [2, 13, 28], in agreement with the early guess of [11]. Similar results have been obtained by [5], [14] and [81].

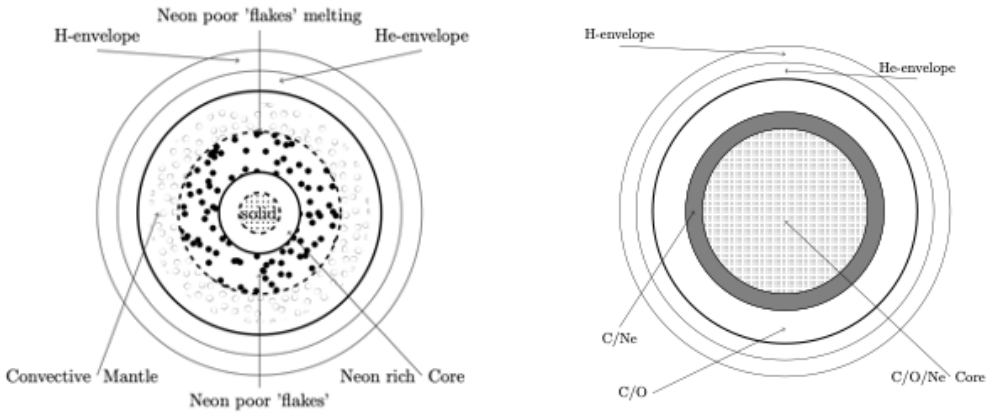

Figure 9: Structure of a C/O/Ne white dwarf during the distillation process of neon.

The sedimentation induced by crystallization of a C/O/Ne mixture is more complex since it depends on the behaviour of a multicomponent diagram that is not well known. In the first attempts to guess the behaviour of ^{22}Ne, this ternary mixture was approached by a binary mixture containing neon and an average isotope between carbon and oxygen. The outcome was the existence of an azeotrope for neon abundances by number in the range of 0.05 to 0.13 [38, 87]. Since the expected abundance of neon is smaller than these values, the resulting solid is lighter than the liquid (Fig. 4) and rises upwards, melting when the solidification temperature, which depends on the density as $T_S \propto \rho^{1/3}$, becomes equal to that of the nearly isothermal core and, depending on their density, this matter re-homogenizes via Rayleigh-Taylor instabilities. Figure 9-left displays the final structure, a core rich in neon (azeotropic composition), that initially is liquid and eventually solidifies without any further compositional change, surrounded by a layer containing raising flakes that are neon poor and a convective mantle with a neon content gradually decreasing[6] [39, 61, 83, 87]. The net effect is a migration of neon towards the central regions and a release of gravitational energy [38, 47].

A second attempt, now taking into account the ternary nature of the mixture, revealed that for normal abundances neon was only playing a minor role in the carbon-oxygen separation, without any change in the abundance of neon, but if the abundance of oxygen was able to reach a low

[6]Notice that as previously mentioned this structure is prone to generate a dynamo much more energetic that in the case of the one associated to the C/O crystallization, or to facilitate the emergence of a previously existing magnetic field [43].

enough value, an off-center solid shell made of carbon and neon without oxygen formed [86]. A more accurate calculation also found that, effectively, depending on the relative abundance of oxygen it was possible to obtain stars with a neon rich core or a carbon-neon shell without oxygen [9]. More precisely, three possibilities were found: a) when the liquid is rich enough in ^{22}Ne, the solid in equilibrium is poor in neon, crystals float and the final outcome is a solid core with a composition (x_C, x_O, x_{Ne}) = (0.8, 0.0, 0.2) by number, surrounded by a C/O mantle free of neon that crystallizes as usual, b) when the central mixture is oxygen poor, the distillation process can proceed and the final outcome is a neon rich core surrounded by a C/O mantle like in case a), and c) when the composition is more or less standard, $x_O = 0.53$, $x_{Ne} = 0.009$ for instance, the distillation process cannot start and the solid has the composition predicted by the C/O mixture without changes in the neon distribution but, since the outer layers are gradually depleted in oxygen, there is a moment at which the distillation starts and the final outcome is a C/O/Ne core, surrounded by a C/Ne shell, both surrounded by a C/O mantle free of neon[7].

The sedimentation of ^{56}Fe can also play an important role [102]. If the hypothesis of an effective binary mixture is adopted, the predicted behaviour is a eutectic behaviour and, since the abundance of this impurity is smaller than the eutectic value, the outcome is a distillation process that creates an iron rich core at the centre [87]. A recent analysis [15] has found that Fe-rich crystals separate before solidification of the rest of the mixture and create an iron rich core that can be made of nearly pure iron or a C/O/Fe alloy, depending on the exact composition of the star. Since this phenomenon occurs very early, concentric shells containing different impurities can form like an Fe-rich core surrounded by a Ne-rich shell and both surrounded by a C/O mantle, for instance.

5. Tools to extract collective properties of white dwarfs

The two main tools to obtain collective information about white dwarfs relays on their distribution in the Hertzsprung-Russell (HR) diagram and on their luminosity function.

The density of stars in a given region of the HR-diagram indicates the existence of a process that slows down their evolution and/or forces them to evolve through this region thus providing information about the properties of these stars. In particular, *GAIA* mission has provided parallaxes with the necessary accuracy for building a detailed HR-diagram of the white dwarf domain [26]. This region (Fig. 10) contains a clear main concentration of stars distributed continuously from left to right, following more or less the constant radius cooling tracks, that has been labelled (A). Just below there is a second nearly parallel concentration labelled (B) that separates in the region $-0.1 \lesssim G_{BP} - G_{RP} \lesssim 0.8$, and a third, weaker concentration, labelled (Q), placed below the two main groups but not following the constant mass evolutionary tracks. It starts around $M_G \sim 13$, $G_{BP} - G_{RP} \sim -0.3$ and merges with A,B groups at $G_{BP} - G_{RP} \sim 0.2$.

At present there is a wide consensus that the A-branch is mainly composed of DA-white dwarfs with a standard mass distribution but the origin of the other two branches is still under discussion.

The B-branch bifurcation, which partially coincides with the 0.8 $M_\odot$ tracks, has been attributed to a flattening of the IFMR in the corresponding region [24] or to the merging of a double white dwarf [53] thus favouring of an excess of white dwarfs around such a mass. Another possibility,

[7]Notice that a tangential collision of two white dwarfs can eject part of this ^{12}C^{22}Ne layer to the ISM providing in this way a new hypothetical scenario to account for the Ne-E anomaly observed in solar meteorites [45, 46]

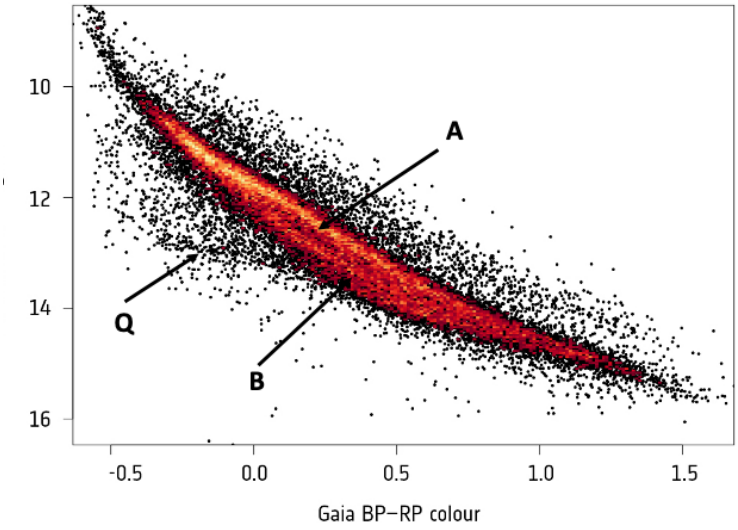

Figure 10: White dwarfs in the HR-diagram (Copyright: ESA/Gaia/DPAC).

however, is the contamination of the atmosphere by small amounts of carbon coming from the outer core that modify the evolutionary path without modifying the mass distribution [10, 12].

The Q-branch is thought to be the consequence of the settling of ^{22}Ne induced by crystallization of massive C/O white dwarfs [14]. This scenario needs single massive white dwarfs made of oxygen with abundance of ^{22}Ne much larger than solar, for which reason a promising scenario is the merging of a white dwarf with a subgiant star [89]. Once more, the metal content plays an important role.

5.1 The luminosity function

The luminosity function of white dwarfs (WDLF) is defined as the number of white dwarfs per unit volume or per unit of Galactic disc surface in the interval $(l, l + dl)$, with $l = -\log_{10}(L/L_\odot)$, per unit of luminosity interval

$$N(l) = \int_{M_{\rm i}(Z)}^{M_{\rm s}(Z)} \Phi(M)\,\Psi[T - t_{\rm cool}(l,m,Z) - t_{\rm PS}(M,Z)]\tau_{\rm cool}(l,m,Z)\;dM \tag{3}$$

where M is the progenitor mass in solar masses, Z is the initial metallicity, and m is the mass of the white dwarf that results from the evolution of a Main Sequence star of mass M. Notice that it is necessary to adopt an IFMR to connect the mass of the white dwarf with the mass of the progenitor. The advantage is that it is not necessary to compute the derivative of this function which is poorly known. Φ is the initial mass function (IMF), Ψ is the star formation rate (SFR), $t_{\rm PS}$ is the lifetime of the progenitor, $t_{\rm cool}$ is the cooling time of the white dwarf at the luminosity l, and $\tau_{\rm cool}$ is the characteristic time at the luminosity l [64].

This luminosity function, averaged over an interval of luminosity Δl, can also be directly computed as follows [48]. Assume a stellar population that forms at a rate $\Psi(t)$. After a time T, the number of white dwarfs that have a luminosity l per unit of luminosity interval is given by

$$N(l,T) = \frac{1}{\Delta l}\int_t\int_M \Phi\,(M)\,\Psi\,(t)\,dMdt \tag{4}$$

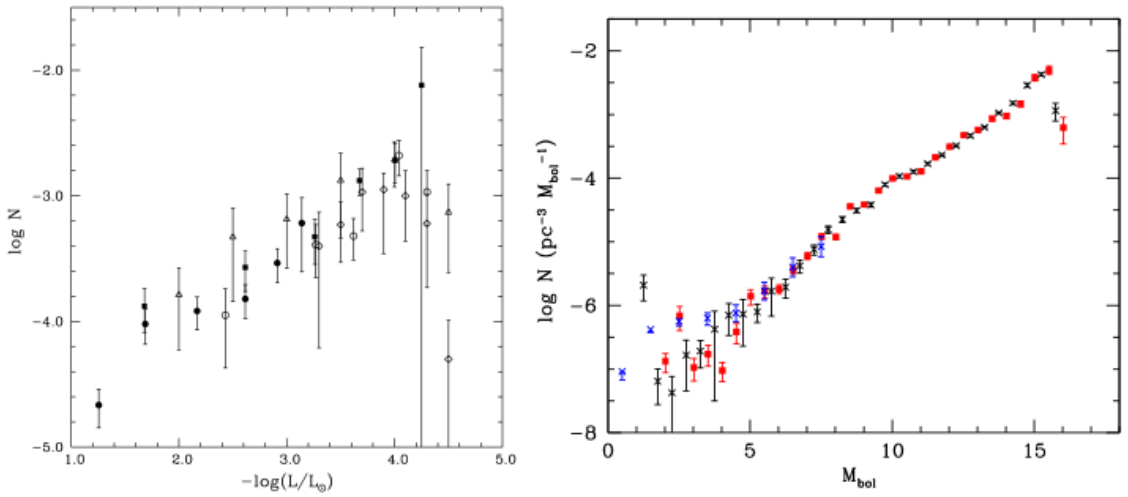

Figure 11: Left: Luminosity functions obtained before the large cosmological surveys – [58], full circles; [25], full squares; [66], open triangles; [57],open diamonds; [54], open circles. Right: Luminosity functions obtained from the SDSS catalogue: Black solid squares [32], open blue squares, only DAs [21], black crosses [56], and green stars [63]. Magenta stars were obtained from the SCSS catalogue [75] and contain DA and non–DA stars.

where, as before, M is the mass of the parent star, and the integral is constrained to the domain

$$T - t_{cool}\,(M, l - 0.5\Delta l) \leq t + t_{MS}\,(M) \leq T - t_{cool}\,(M, l + 0.5\Delta l) \tag{5}$$

for all the stars able to produce a white dwarf.

Notice, however, that both formulations of the luminosity function assume that the number of stars is conserved, which is not strictly correct. On one hand there are radial and vertical motions that inject and remove stars from the solar neighborhood and, on another hand, a fraction of white dwarfs in binaries can be destroyed via supernova explosion or merge to form a unique white dwarf which, in some cases, can explode.

The first empirical luminosity function was obtained by Weidemann [100] and was improved by several authors during nineties (Figure 11, left) proving in this way that the evolution of white dwarfs was just a cooling process and that there was a cut-off in the distribution caused by the finite age of the Galaxy. The position of the cut-off is sensitive to the cooling rate and, consequently, it can be used to constrain theoretical models or the age of the Galaxy. However the low number of stars in the samples, few hundreds, and the uncertainties in the position of the cut-off prevented anything else that obtaining upper bounds.

The advent of large cosmological surveys like the Sloan Digital Sky Survey (SDSS) and the Super COSMOS Sky Survey (SCSS), both completely independent, introduced a noticeable improvement in the precision and accuracy of the luminosity function since they allowed to increase the sample size to several thousands of stars. Figure 11-right, displays both functions normalized to

the $M_{\rm bol} \approx 12$ bin. As can be seen, they nearly coincide over a large part of the brightness interval. At large brightness, $M_{\rm bol} < 6$, both luminosity functions show a large dispersion, not plotted in the figure, as a consequence of the fact that the proper motion method is not appropriate there. One way to circumvent this problem relies on the UV-excess technique [56]. The results obtained in this way are represented by black crosses after matching their dim region with the corresponding bright segment of the Harris et al. [32] distribution. The discrepancies at low luminosities are due to the difficulty of separating DAs from non-DAs and to the different behaviour of the envelope. As a complement, the luminosity function of the dimmest white dwarfs obtained by Leggett et al. [57] has been included (red triangles).

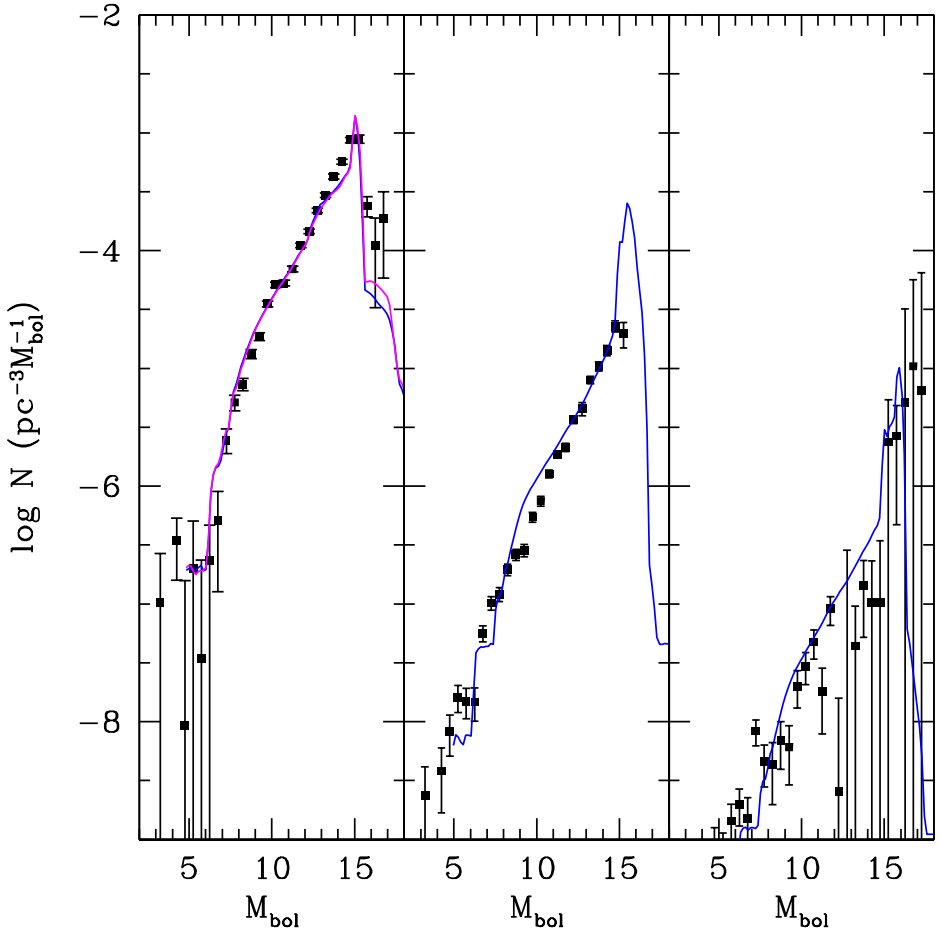

Figure 12: From left to right, luminosity functions of DA and non-DA white dwarfs from the SCSS catalogue for the thin and thick disks, and the halo [75].

The luminosity function depends not only on the properties of white dwarfs but also on the properties of the Galaxy via SFR and IMF (Eqs. 3 and 4). This degeneracy can be removed assuming the universality of the IMF and considering the luminosity functions of populations that have different star formation histories since the signature of any intrinsic property of white dwarfs will appear in all the luminosity functions at roughly the same bolometric magnitude. The accuracy

of both catalogues, SCSS and SDSS, has been enough to allow building preliminary luminosity functions of the thin and thick disks and the halo (Fig. 12) using kinematic arguments [63, 75]. The blue line of the halo WDLF has been obtained assuming a constant burst of star formation that lasted from 0 to 1.4 Gyr at the beginning of the formation of the Galaxy (age 13.4 Gyr) and a metallicity $Z = 2 \times 10^{-5}$, that of the thick disk was obtained assuming a constant SFR lasting from 0 to 4 Gyr and $Z = 2 \times 10^{-3}$ and that of the thin disk also assuming a constant SFR from 4 Gyr to present, and solar metallicity (blue line) or time dependent metallicity (magenta line) according to the Twarog [95] recipy. All of them were normalized to the region around $M_{\rm bol} \simeq 12$, and using the BaSTI models [81] which take into account the gravitational settling of neon, but not the distillation process. It is evident that accurate and precise luminosity functions together with improved theoretical models will provide in a next future new information about these structures.

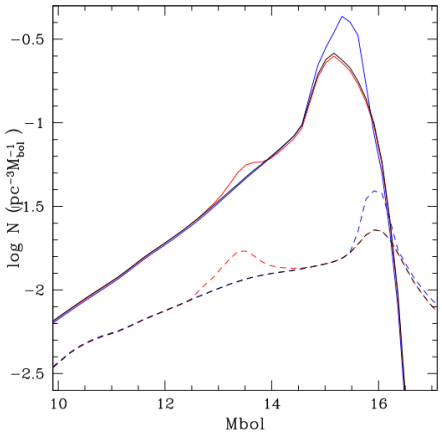

Figure 13: Luminosity functions obtained with SFR constant (black), adding a young, 2 Gyr, burst (red) or an old. 11 Gyr, burst (blue), normalized to $M_{bol} = 13$. Dashed lines have the same meaning but restricted to the mass range 0.9-11 $M_\odot$

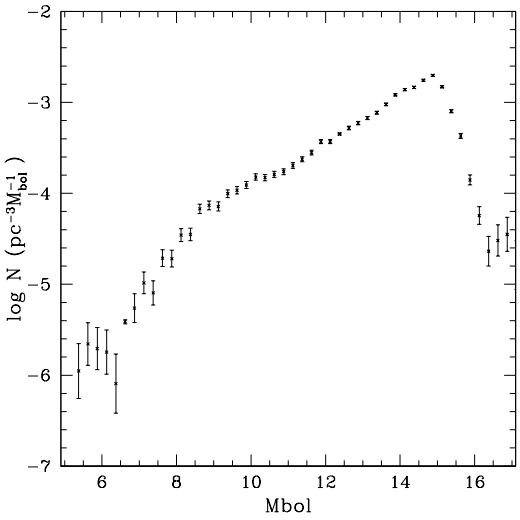

Figure 14: Luminosity function obtained with the 100 pc sample of white dwarfs in the*Gaia* Catalogue of Nearby Stars (GCNS) with bins of 0.25 $M_{\rm bol}$. The structure and features are statistically significant for all bins excepting the first and the last ones [27].

The quality of this new luminosity functions allowed, for the first time, to determine their shape and to use the slope as a tool to test new physical theories. This can be understood in the following way, Eq. 3 can be written as:

$$n\,(l) \propto \langle \tau_{cool} \rangle \int_{M_i}^{M_{\rm max}} \Phi\,(M)\,\Psi\left(T_G - t_{cool} - t_{ps}\right) dM \qquad (6)$$

If this equation is restricted to the branch of bright white dwarfs, i.e. those for which $t_{\rm cool}$ is small, the lower limit of the integral is satisfied by low-mass stars and, as a consequence of the strong dependence of the main sequence lifetimes with mass, it adopts a value that is almost independent of the luminosity under consideration. Therefore, if Ψ is a well-behaved function and T_G is large enough, the lower limit is almost independent of the luminosity, and the value of the integral is

incorporated into the normalization constant in such a way that the shape of the luminosity function only depends on the averaged physical properties of white dwarfs [37]. This average is dominated by low mass white dwarfs and, as far as the mass spectrum is not strongly perturbed by the adopted star formation or the initial mass function, it is representative of the intrinsic properties of white dwarfs [41]. This shape, however, can be modified by a recent burst of star formation since, in this case, low-mass main sequence stars have no time to become white dwarfs and M_I in Eq. 6 becomes luminosity dependent. On the contrary, if the burst is old enough, the corresponding bright branch of the luminosity functions are barely modified (Fig. 13). Therefore, if an additional source or sink of energy is added, the characteristic cooling time is modified and its imprint appears in the luminosity function, as can be seen in Figure 11-right, where a change of slope is evident at magnitudes $M_{\rm bol} \sim 8$. This change is caused by the transition from a cooling dominated by neutrinos to one dominated by photons. As an example, this technique was used by Isern et al. [40] to suggest that axions of the DFSZ type could be contributing to the cooling of white dwarfs.

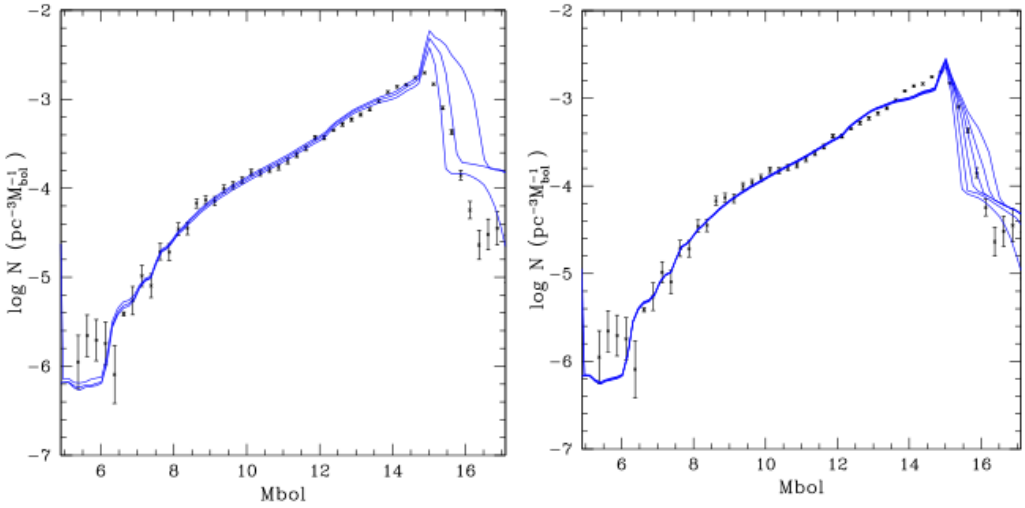

Figure 15: Theoretical luminosity functions taking into account the metallicity effects for ages of 8, 10, and 12 Gyr (left) and the same but taking into account the increase of the height scale of older objects for ages of 8, 9, 10, 11, 12 and 13 Gyr (right).

The previously mentioned WDLFs were built using the theoretical mass-radius relationship, which is still rather uncertain, and parallaxes obtained before *Gaia*. The high accuracy of parallaxes and photometric data provided by *Gaia* [26, 27] has allowed to increase the number of high-confidence white dwarfs candidates by more than one order of magnitude, being at present of the order $\sim 360,000$ stars [29, 30, 51]. In particular, the *Gaia* Catalogue of Nearby Stars (GCNS) has allowed to obtain a luminosity function (Fig. 14) representative of white dwarfs within a distance of 100 pc with bins of 0.25 $M_{\rm bol}$ [27]. The GCNS is reliable and complete within a well defined survey volume and allows to identify WDs from their position in the HR-diagram. Although the sample is volume limited, the luminosity function displayed in Figure 14 has been corrected using the $1/V_{max}$ method to avoid the biases introduced by the scale height above the Galactic plane and the low luminosity of white dwarfs as compared with the limiting apparent magnitude of *Gaia*.

Figure 15, left, displays the theoretical luminosity function adopting the BaSTI models, the time-dependent metallicity of Twarog, op.cit., a constant star formation rate and normalizing around $M_{\rm bol} = 12$. As it can be seen the qualitative agreement is rather good except in the regions $8 \lesssim M_{\rm bol} \lesssim 10$, $13 \lesssim M_{\rm bol} \lesssim 15$, and the peak. The first one may be caused by a burst, old $\sim 0.5 - 0.7$ Gyr, in the SFR [93], while the second region is affected by the hypothetical distillation of ^{22}Ne and deserves more attention. The discrepancies in the region of the peak can be noticeably reduced if it is taken into account that older objects have higher scale heights above the galactic plane. This figure (right) also displays the results of introducing a variable scale height like that of Mira stars [101].

5.2 The luminosity function of massive white dwarfs

Thanks to the *Gaia* data it has been possible to build a reliable and precise luminosity function of massive white dwarfs in the solar neighbourhood, $d \lesssim 100$ pc [94] (Fig. 16, left panel). If the luminosity function, Eq. 3, is restricted to massive white dwarfs, i.e. those for which it is possible to neglect the lifetime of the progenitor in front of the cooling time, and $\Psi(t)$ is smooth enough[8], then

$$N(l,T) \simeq \frac{\langle \Psi \rangle}{\Delta l} \int_{\Delta M} \Phi\,(M)\,\Delta t_{cool}\,(l,M)\,dM \tag{7}$$

with

$$\Delta t_{cool} = t_{cool}\,(l + 0.5\Delta l, M) - t_{cool}\,(l - 0.5\Delta l, M) \tag{8}$$

and consequently, the age and with of any bin and the star formation rate corresponding to this time can be computed as

$$\langle t \rangle = \frac{\int_{\Delta M} \Phi(M) t dM}{\int_{\Delta M} \Phi(M) dM} \tag{9}$$

$$\langle \Delta t \rangle = \frac{\int_{\Delta M} \Phi(M) \Delta t dM}{\int_{\Delta M} \Phi(M) dM} \tag{10}$$

$$\langle \Psi \rangle = \frac{N(l,T)\Delta l}{\int_{\Delta M} \Phi\,(M)\,\Delta t_{cool}\,(l,M)\,dM} \tag{11}$$

It is important to notice here that the star formation rate obtained in this way is an effective one in the sense that it recovers the present age distribution of the sample, but does not take into account the secular evolution of the sample mainly due to radial migrations and height inflation. On another hand, hidden white dwarfs in binaries and non-resolved double degenerates can bias the sample, while double degenerate mergers can reduce the density of white dwarfs in some bins and, in the case they do not explode as SNIa, reappear as newly born hot single white dwarfs with the corresponding density increase of younger bins, thus modifying the SFR deduced from these data. The importance of this effect is small given the present level of precision, but it is necessary to include it in order to interpret future high precision WDLFs.

[8]This method is also valid for white dwarfs with masses within a limited enough range of values.

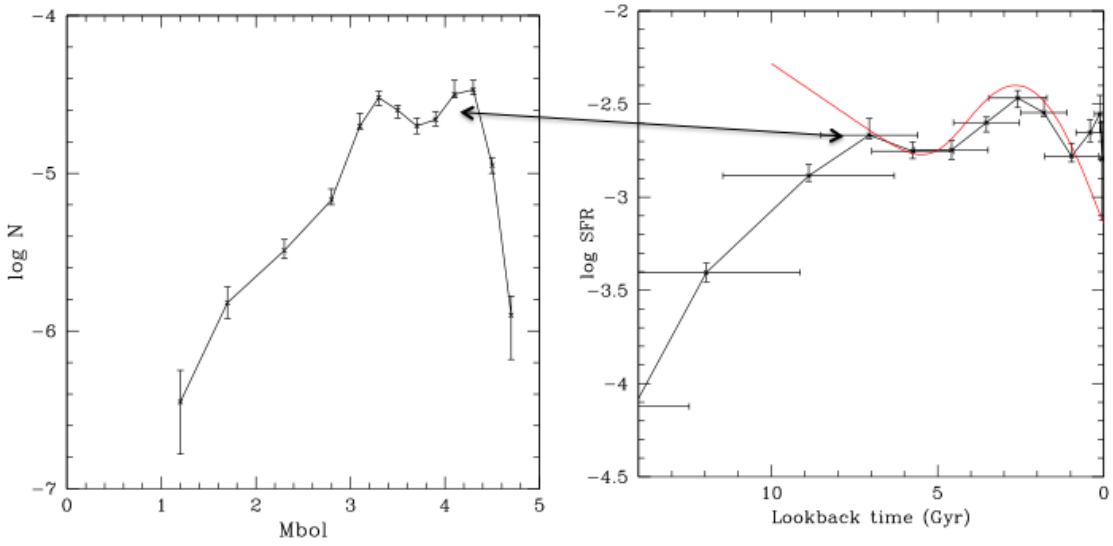

Figure 16: Left panel: empirical luminosity function of massive ($0.9 \leq M_{\rm WD}/M_\odot \leq 1.1$) DA white dwarfs in the solar neighbourhood [94]. Right panel: in black, the corresponding star formation rate [44], in red, the Galactic disc star formation rate [62].

The star formation rate obtained in this way is not constant or monotonically decreasing as it is often assumed. It grew quickly in the past, during the first epochs of the Galaxy, it roughly stabilized and started to decrease 7 to 6 Gyr ago. A noticeable feature is a prominent peak centred around 2.5 Gyr ago, the exact position being model depending. This means that the result may be dependent of the treatment of the metal content.

The existing degeneracy between galactic properties and evolutionary models implies that different stellar models can lead to different star formation histories, for which reason it is necessary to compare these results with others obtained independently. Mor et al. [62] computed the star formation history of the Galactic disk using main sequence stars from the Gaia DR2 and the Besançon Galaxy Model. Since this function is expressed in stars per unit of disk surface it has been divided by an arbitrary and constant height scale above the galactic plane (red line, Fig. 16-right). As it can be seen both methods, local and galactic, predict a concordant burst of star formation $\sim$ 2.5 Gyr ago but diverge at early times. This divergence may have several origins, a local delay in starting the star formation process[9], a different behaviour of the outer and inner disks, a vertical dilution caused by a galaxy collision or just the conversion of DA white dwarfs into non-DAs. The peak that appears at $\sim 0.2 - 0.5$ Gyr is in the limit of applicability of the method and deserves more attention since it could be related with the burst quoted by Tononi et al. [93].

A possible source of uncertainty is the role played by mergers The majority of stars are part

[9]White dwarf data are representative of the local neighbourhood while the Mor's result is representative of a large fraction of the Galactic disk.

of binary or multiple stellar systems and in the case of white dwarfs in binaries with short enough periods both components can interact and explode or even merge. In the first case, a supernova explosion implies the destruction of one or two white dwarfs depending on the adopted scenario, single or double degenerate events. However, given the scarcity of Type Ia supernovae as compared with the total number of white dwarfs, its impact on the luminosity function is probably low, at least within the present uncertainties. Mergers are more relevant since in these events two stars are removed and a new one, hot and massive, is created thus contaminating the sub-sample of massive white dwarfs. It is evident that white dwarfs in such systems have a different evolutionary path than the single ones and need a different treatment [70, 85]. An obvious question is how to distinguish single white dwarfs that have a binary origin from those that were born single. It has been claimed that they could be separated thanks to the distribution of rotation velocities since it is expected that those coming from a merger have higher angular velocities, but the problem is that the evolution of the angular momentum is not well known. The mass distribution can also be used since these objects are biased towards higher values, perhaps larger than 0.8 $M_\odot$ but the problem is that the relationship between the mass of the progenitor and the mass of the white dwarf is not well known in the case of singles and, as it has been seen, it depends on the metallicity.

5.3 The luminosity function of white dwarfs in non interacting binaries

Probably the best way to tackle the problem of the influence of metals in the luminosity function is to consider non-interacting binary systems containing a white dwarf and a non-degenerate star since the last one can provide the initial metallicity of the system. The number of binaries born per unit time with masses M_1 and M_2 at the galactic time t and initial separation A_0 in a region of the Galaxy is

$$b(M_1, q, A_0, t) = \Psi_B(t)\Phi(M_1)f(q)H_0(A_0) \tag{12}$$

where Ψ_B is the mass converted into binary stars per unit time, $f(q)$ is the mass ratio distribution with $q = M_2/M_1 \leq 1$, and H_0 is the initial distribution of separations.

The luminosity function of white dwarfs that are members of a non-interacting binary system in which the companion is a non-degenerate star can be computed as before as

$$N_B(M_{bol}, T_G) = \frac{1}{\Delta M_{bol}} \int_t \int_{M_1} \int_q \int_{A_0} b(M_1, q, A_0, t) dt dM_1 dq dA_0 \tag{13}$$

with the following constraints

$$t + t_{PS}[M_1, Z(t)] + t_{cool}[m_{wd}, Z(t), M_{bol} - 0.5\Delta M_{bol}] = T_G \tag{14}$$

$$t + t_{PS}[M_1, Z(t)] + t_{cool}[m_{wd}, Z(t), M_{bol} + 0.5\Delta M_{bol}] = T_G \tag{15}$$

for each $0 \leq t \leq T_G$. Since the metallicity has to be provided by the non-degenerate companion, an additional constrain has to be introduced to guarantee that the secondary has not reached yet a white dwarf status,

$$t + t_{MS}(qM_1, Z) > T_G \tag{16}$$

where $t_{MS}(qM_1, Z)$ is the lifetime of the secondary.

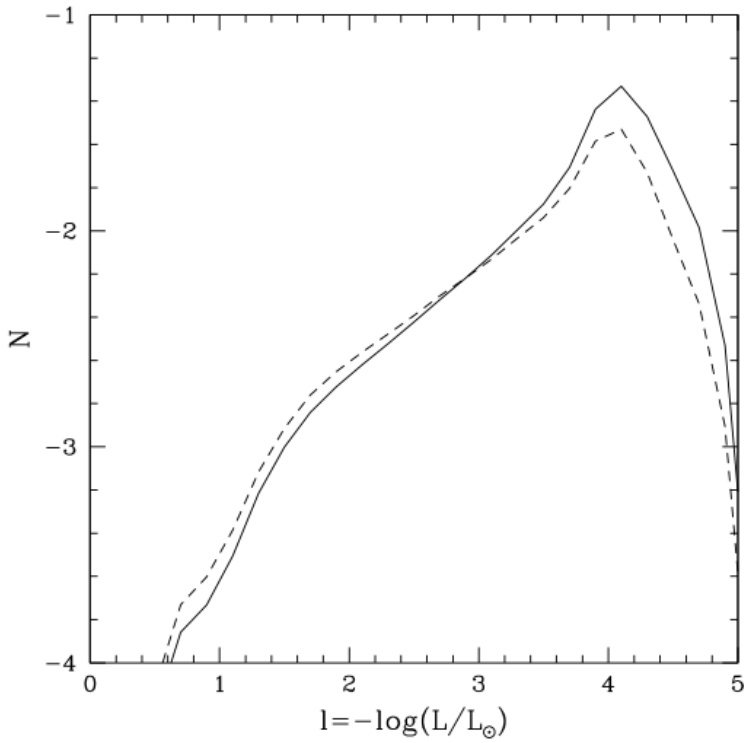

Figure 17: Luminosity function of white dwarfs in non-interacting binaries (solid line) and single (dashed line). Both have been obtained assuming a constant SFR and solar metallicity and have been normalized to $l = 3$.

As expected, the WDLF (Fig. 17) is not strongly modified by the introduction of Eq. 16 and has the advantage that provides at the same time a reliable luminosity function and a time dependent distribution of metals in the solar neighbourhood which at the same time allows to refine the luminosity function of single white dwarfs.

6. Conclusions

Gaia is producing a set of highly accurate and precise fundamental data like trigonometric parallaxes, luminosities, colours and spectral characteristics that is completely changing our view about many stellar types and the structure of the Galaxy. In the case of white dwarfs, these data ha allowed to obtain a fine picture of they distribution in the HR-diagram and an accurate luminosity function that are allowing to better understand the properties of such stars.

An ingredient that is still lacking is the metallicity of the parent star as a consequence of their strong gravitational field that rapidly erases any vestige of the initial metal content. Its role, as it has been seen, is important to understand many aspects of the evolution of these stars and to use them as reliable chronometers.

Acknowledgements

This work has been funded by the Spanish Ministry of Science and Innovation and FEDER UE (MCI-AEI-FEDER) the program Unidad de Excelencia María de Maeztu CEX2020-001058-M, and the program 2021-SGR-1526 (Generalitat de Catalunya), and by the Munich Institute for Astro-, Particle and BioPhysics (MIAPbP), which is funded by the Deutsche Forschungsgemeinschaft (DFG, German Research Foundation) under Germany´s Excellence Strategy – EXC-2094 – 390783311.

References

[1] L. G. Althaus, A. H. Córsico, J. Isern, and E. García-Berro. Evolutionary and pulsational properties of white dwarf stars. *A&A Rev.*, 18:471–566, October 2010. doi: 10.1007/s00159-010-0033-1.

[2] L. G. Althaus, E. García-Berro, I. Renedo, J. Isern, A. H. Córsico, and R. D. Rohrmann. Evolution of White Dwarf Stars with High-metallicity Progenitors: The Role of ^{22}Ne Diffusion. *ApJ*, 719(1):612–621, August 2010. doi: 10.1088/0004-637X/719/1/612.

[3] Jeff J. Andrews, Marcel A. Agüeros, A. Gianninas, Mukremin Kilic, Saurav Dhital, and Scott F. Anderson. Constraints on the Initial-Final Mass Relation from Wide Double White Dwarfs. *ApJ*, 815(1):63, December 2015. doi: 10.1088/0004-637X/815/1/63.

[4] Manuel Barrientos and Julio Chanamé. Improved Constraints on the Initial-to-final Mass Relation of White Dwarfs Using Wide Binaries. *ApJ*, 923(2):181, December 2021. doi: 10.3847/1538-4357/ac2f49.

[5] Evan B. Bauer, Josiah Schwab, Lars Bildsten, and Sihao Cheng. Multi-gigayear White Dwarf Cooling Delays from Clustering-enhanced Gravitational Sedimentation. *ApJ*, 902(2):93, October 2020. doi: 10.3847/1538-4357/abb5a5.

[6] Lars Bildsten and David M. Hall. Gravitational Settling of ^{22}NE in Liquid White Dwarf Interiors. *ApJ*, 549(2):L219–L223, March 2001. doi: 10.1086/319169.

[7] Simon Blouin, Jérôme Daligault, Didier Saumon, Antoine Bédard, and Pierre Brassard. Toward precision cosmochronology. A new C/O phase diagram for white dwarfs. *A&A*, 640:L11, August 2020. doi: 10.1051/0004-6361/202038879.

[8] Simon Blouin, Nathaniel R. Shaffer, Didier Saumon, and Charles E. Starrett. New Conductive Opacities for White Dwarf Envelopes. *ApJ*, 899(1):46, August 2020. doi: 10.3847/1538-4357/ab9e75.

[9] Simon Blouin, Jérôme Daligault, and Didier Saumon. ^{22}Ne Phase Separation as a Solution to the Ultramassive White Dwarf Cooling Anomaly. *ApJ*, 911(1):L5, April 2021. doi: 10.3847/2041-8213/abf14b.

[10] Simon Blouin, Antoine Bédard, and Pier-Emmanuel Tremblay. Carbon dredge-up required to explain the Gaia white dwarf colour-magnitude bifurcation. *MNRAS*, 523(3):3363–3375, August 2023. doi: 10.1093/mnras/stad1574.

[11] E. Bravo, J. Isern, R. Canal, and J. Labay. On the contribution of Ne-22 to the synthesis of Fe-54 and Ni-58 in thermonuclear supernovae. *A&A*, 257(2):534–538, April 1992.

[12] Maria Camisassa, Santiago Torres, Mark Hollands, Detlev Koester, Roberto Raddi, Leandro G. Althaus, and Alberto Rebassa-Mansergas. A hidden population of white dwarfs with atmospheric carbon traces in the Gaia bifurcation. *A&A*, 674:A213, June 2023. doi: 10.1051/0004-6361/202346628.

[13] María E. Camisassa, Leandro G. Althaus, Alejandro H. Córsico, Núria Vinyoles, Aldo M. Serenelli, Jordi Isern, Marcelo M. Miller Bertolami, and Enrique García–Berro. The Effect of ^{22}NE Diffusion in the Evolution and Pulsational Properties of White Dwarfs with Solar Metallicity Progenitors. *ApJ*, 823(2):158, June 2016. doi: 10.3847/0004-637X/823/2/158.

[14] María E. Camisassa, Leandro G. Althaus, Santiago Torres, Alejandro H. Córsico, Alberto Rebassa-Mansergas, Pier-Emmanuel Tremblay, Sihao Cheng, and Roberto Raddi. Forever young white dwarfs: When stellar ageing stops. *A&A*, 649:L7, May 2021. doi: 10.1051/0004-6361/202140720.

[15] M. E. Caplan, I. F. Freeman, C. J. Horowitz, A. Cumming, and E. P. Bellinger. Cooling Delays from Iron Sedimentation and Iron Inner Cores in White Dwarfs. *ApJ*, 919(1):L12, September 2021. doi: 10.3847/2041-8213/ac1f99.

[16] S. Cassisi, A. Y. Potekhin, A. Pietrinferni, M. Catelan, and M. Salaris. Updated Electron-Conduction Opacities: The Impact on Low-Mass Stellar Models. *ApJ*, 661(2):1094–1104, June 2007. doi: 10.1086/516819.

[17] S. Catalán, J. Isern, E. García-Berro, and I. Ribas. The initial-final mass relationship of white dwarfs revisited: effect on the luminosity function and mass distribution. *MNRAS*, 387:1693–1706, July 2008. doi: 10.1111/j.1365-2966.2008.13356.x.

[18] Tim Cunningham, Pier-Emmanuel Tremblay, and Mairi W. O'Brien. Initial-final mass relation from white dwarfs within 40 pc. *MNRAS*, 527(2):3602–3611, January 2024. doi: 10.1093/mnras/stad3275.

[19] Francesca D'Antona and Italo Mazzitelli. The Fastest Evolving White Dwarfs. *ApJ*, 347: 934, December 1989. doi: 10.1086/168185.

[20] F. C. De Gerónimo, L. G. Althaus, A. H. Córsico, A. D. Romero, and S. O. Kepler. Asteroseismology of ZZ Ceti stars with fully evolutionary white dwarf models. I. The impact of the uncertainties from prior evolution on the period spectrum. *A&A*, 599:A21, March 2017. doi: 10.1051/0004-6361/201629806.

[21] S. DeGennaro, T. von Hippel, D. E. Winget, S. O. Kepler, A. Nitta, D. Koester, and L. Althaus. White Dwarf Luminosity and Mass Functions from Sloan Digital Sky Survey Spectra. *AJ*, 135:1–9, January 2008. doi: 10.1088/0004-6256/135/1/1.

[22] Christopher J. Deloye and Lars Bildsten. Gravitational Settling of ^{22}Ne in Liquid White Dwarf Interiors: Cooling and Seismological Effects. *ApJ*, 580(2):1077–1090, December 2002. doi: 10.1086/343800.

[23] P. D. Dobbie, R. Napiwotzki, M. R. Burleigh, M. A. Barstow, D. D. Boyce, S. L. Casewell, R. F. Jameson, I. Hubeny, and G. Fontaine. New Praesepe white dwarfs and the initial mass-final mass relation. *MNRAS*, 369(1):383–389, June 2006. doi: 10.1111/j.1365-2966.2006.10311.x.

[24] Kareem El-Badry, Hans-Walter Rix, and Daniel R. Weisz. An Empirical Measurement of the Initial-Final Mass Relation with Gaia White Dwarfs. *ApJ*, 860(2):L17, June 2018. doi: 10.3847/2041-8213/aaca9c.

[25] D. W. Evans. The APM Proper Motion Project. I - High proper motion stars. *MNRAS*, 255:521–538, April 1992. doi: 10.1093/mnras/255.3.521.

[26] Gaia Collaboration, C. Babusiaux, F. van Leeuwen, M. A. Barstow, and et al. Gaia Data Release 2. Observational Hertzsprung-Russell diagrams. *A&A*, 616:A10, August 2018. doi: 10.1051/0004-6361/201832843.

[27] Gaia Collaboration, R. L. Smart, L. M. Sarro, J. Rybizki, and et al. Gaia Early Data Release 3. The Gaia Catalogue of Nearby Stars. *A&A*, 649:A6, May 2021. doi: 10.1051/0004-6361/202039498.

[28] E. García-Berro, L. G. Althaus, A. H. Córsico, and J. Isern. Gravitational Settling of ^{22}Ne and White Dwarf Evolution. *ApJ*, 677(1):473–482, April 2008. doi: 10.1086/527536.

[29] N. P. Gentile Fusillo, P. E. Tremblay, E. Cukanovaite, A. Vorontseva, R. Lallement, M. Hollands, B. T. Gänsicke, K. B. Burdge, J. McCleery, and S. Jordan. A catalogue of white dwarfs in Gaia EDR3. *MNRAS*, 508(3):3877–3896, December 2021. doi: 10.1093/mnras/stab2672.

[30] Nicola Pietro Gentile Fusillo, Pier-Emmanuel Tremblay, Boris T. Gänsicke, Christopher J. Manser, Tim Cunningham, Elena Cukanovaite, Mark Hollands, Thomas Marsh, Roberto Raddi, Stefan Jordan, Silvia Toonen, Stephan Geier, Martin Barstow, and Jeffrey D. Cummings. A Gaia Data Release 2 catalogue of white dwarfs and a comparison with SDSS. *MNRAS*, 482(4):4570–4591, February 2019. doi: 10.1093/mnras/sty3016.

[31] N. Giammichele, S. Charpinet, G. Fontaine, P. Brassard, E. M. Green, V. Van Grootel, P. Bergeron, W. Zong, and M. A. Dupret. A large oxygen-dominated core from the seismic cartography of a pulsating white dwarf. *Nature*, 554(7690):73–76, February 2018. doi: 10.1038/nature25136.

[32] H. C. Harris, J. A. Munn, M. Kilic, J. Liebert, K. A. Williams, T. von Hippel, S. E. Levine, D. G. Monet, D. J. Eisenstein, S. J. Kleinman, T. S. Metcalfe, A. Nitta, D. E. Winget, J. Brinkmann, M. Fukugita, G. R. Knapp, R. H. Lupton, J. A. Smith, and D. P. Schneider. The White Dwarf Luminosity Function from Sloan Digital Sky Survey Imaging Data. *AJ*, 131:571–581, January 2006. doi: 10.1086/497966.

[33] M. Hernanz, E. Garcia-Berro, J. Isern, R. Mochkovitch, L. Segretain, and G. Chabrier. The influence of crystallization on the luminosity function of white dwarfs. *ApJ*, 434:652–661, October 1994. doi: 10.1086/174767.

[34] C. J. Horowitz, A. S. Schneider, and D. K. Berry. Crystallization of Carbon-Oxygen Mixtures in White Dwarf Stars. *Phys. Rev. Lett.*, 104(23):231101, June 2010. doi: 10.1103/PhysRevLett.104.23110110.48550/arXiv.1005.2441.

[35] Jr. Iben, I. and A. V. Tutukov. Cooling of low-mass carbon-oxygen dwarfs from the planetary nucleus stage through the crystallization stage. *ApJ*, 282:615–630, July 1984. doi: 10.1086/162241.

[36] Setsuo Ichimaru, Hiroshi Iyetomi, and Shuji Ogata. Freezing Transition and Phase Diagram of Dense Carbon-Oxygen Mixtures in White Dwarfs. *ApJ*, 334:L17, November 1988. doi: 10.1086/185303.

[37] J. Isern and E. García-Berro. White dwarfs as physics laboratories: the axion case. *Mem. Soc. Astron. Italiana*, 79:545, January 2008.

[38] J. Isern, M. Hernanz, R. Mochkovitch, and E. Garcia-Berro. The role of the minor chemical species in the cooling of white dwarfs. *A&A*, 241:L29–L32, January 1991.

[39] J. Isern, E. García-Berro, M. Hernanz, and G. Chabrier. The Energetics of Crystallizing White Dwarfs Revisited Again. *ApJ*, 528:397–400, January 2000. doi: 10.1086/308153.

[40] J. Isern, E. García-Berro, S. Torres, and S. Catalán. Axions and the Cooling of White Dwarf Stars. *ApJ*, 682(2):L109, August 2008. doi: 10.1086/591042.

[41] J. Isern, S. Catalán, E. García-Berro, and S. Torres. Axions and the white dwarf luminosity function. In *Journal of Physics Conference Series*, volume 172 of *Journal of Physics Conference Series*, page 012005, June 2009. doi: 10.1088/1742-6596/172/1/012005.

[42] J. Isern, A. Artigas, and E. García-Berro. White dwarf cooling sequences and cosmochronology. In *European Physical Journal Web of Conferences*, volume 43 of *European Physical Journal Web of Conferences*, page 05002, March 2013. doi: 10.1051/epjconf/20134305002.

[43] J. Isern, E. García-Berro, B. Külebi, and P. Lorén-Aguilar. Magnetic Fields and the Crystallization of White Dwarfs. In P. E. Tremblay, B. Gaensicke, and T. Marsh, editors, *20th European White Dwarf Workshop*, volume 509 of *Astronomical Society of the Pacific Conference Series*, page 409, March 2017.

[44] Jordi Isern. The Star Formation History in the Solar Neighborhood as Told by Massive White Dwarfs. *ApJ*, 878(1):L11, June 2019. doi: 10.3847/2041-8213/ab238e.

[45] Jordi Isern and Eduardo Bravo. White Dwarf Collisions, a Promising Scenario to Account for Meteoritic Anomalies. *Research Notes of the American Astronomical Society*, 2(3):157, September 2018. doi: 10.3847/2515-5172/aadd50.

[46] Jordi Isern and Eduardo Bravo. White dwarf collisions and the meteoritic Ne-E annomaly. *arXiv e-prints*, art. arXiv:1809.08789, September 2018. doi: 10.48550/arXiv.1809.08789.

[47] Jordi Isern, Enrique García-Berro, Margarida Hernanz, and Robert Mochkovitch. The physics of white dwarfs. *Journal of Physics Condensed Matter*, 10(49):11263–11272, December 1998. doi: 10.1088/0953-8984/10/49/015.

[48] Jordi Isern, Enrique García-Berro, Margarida Hernanz, Robert Mochkovitch, and Santiago Torres. The Halo White Dwarf Population. *ApJ*, 503(1):239–246, August 1998. doi: 10.1086/305977.

[49] Jordi Isern, Enrique García-Berro, Baybars Külebi, and Pablo Lorén-Aguilar. A Common Origin of Magnetism from Planets to White Dwarfs. *ApJ*, 836(2):L28, February 2017. doi: 10.3847/2041-8213/aa5eae.

[50] Adam S. Jermyn, Josiah Schwab, Evan Bauer, F. X. Timmes, and Alexander Y. Potekhin. Skye: A Differentiable Equation of State. *ApJ*, 913(1):72, May 2021. doi: 10.3847/1538-4357/abf48e.

[51] F. M. Jiménez-Esteban, S. Torres, A. Rebassa-Mansergas, G. Skorobogatov, E. Solano, C. Cantero, and C. Rodrigo. A white dwarf catalogue from Gaia-DR2 and the Virtual Observatory. *MNRAS*, 480(4):4505–4518, November 2018. doi: 10.1093/mnras/sty2120.

[52] Jasonjot S. Kalirai, Brad M. S. Hansen, Daniel D. Kelson, David B. Reitzel, R. Michael Rich, and Harvey B. Richer. The Initial-Final Mass Relation: Direct Constraints at the Low-Mass End. *ApJ*, 676(1):594–609, March 2008. doi: 10.1086/527028.

[53] Mukremin Kilic, N. C. Hambly, P. Bergeron, C. Genest-Beaulieu, and N. Rowell. Gaia reveals evidence for merged white dwarfs. *MNRAS*, 479(1):L113–L117, September 2018. doi: 10.1093/mnrasl/sly110.

[54] R. A. Knox, M. R. S. Hawkins, and N. C. Hambly. A survey for cool white dwarfs and the age of the Galactic disc. *MNRAS*, 306:736–752, July 1999. doi: 10.1046/j.1365-8711.1999.02625.x.

[55] D. Koester and D. Schoenberner. Evolution of white dwarfs. *Astron. Astrop.*, 154:125–134, January 1986.

[56] J. Krzesinski, S. J. Kleinman, A. Nitta, S. Hügelmeyer, S. Dreizler, J. Liebert, and H. Harris. A hot white dwarf luminosity function from the Sloan Digital Sky Survey. *A&A*, 508:339–344, December 2009. doi: 10.1051/0004-6361/200912094.

[57] S. K. Leggett, M. T. Ruiz, and P. Bergeron. The Cool White Dwarf Luminosity Function and the Age of the Galactic Disk. *ApJ*, 497:294–302, April 1998. doi: 10.1086/305463.

[58] J. Liebert, C. C. Dahn, and D. G. Monet. The luminosity function of white dwarfs. *ApJ*, 332:891–909, September 1988. doi: 10.1086/166699.

[59] Paola Marigo. The Initial-Final Mass Relation of White Dwarfs: A Tool to Calibrate the Third Dredge-Up. *Universe*, 8(4):243, April 2022. doi: 10.3390/universe8040243.

[60] Zach Medin and Andrew Cumming. Crystallization of classical multicomponent plasmas. *Phys. Rev. E*, 81(3):036107, March 2010. doi: 10.1103/PhysRevE.81.036107.

[61] R. Mochkovitch. Freezing of a carbon-oxygen white dwarf. *A&A*, 122(1-2):212–218, June 1983.

[62] R. Mor, A. C. Robin, F. Figueras, S. Roca-Fàbrega, and X. Luri. Gaia DR2 reveals a star formation burst in the disc 2-3 Gyr ago. *arXiv e-prints*, January 2019.

[63] Jeffrey A. Munn, Hugh C. Harris, Ted von Hippel, Mukremin Kilic, James W. Liebert, Kurtis A. Williams, Steven DeGennaro, Elizabeth Jeffery, Kyra Dame, A. Gianninas, and Warren R. Brown. A Deep Proper Motion Catalog Within the Sloan Digital Sky Survey Footprint. II. The White Dwarf Luminosity Function. *AJ*, 153(1):10, January 2017. doi: 10.3847/1538-3881/153/1/10.

[64] Hye-Rim Noh and John Scalo. History of the Milky Way Star Formation Rate from the White Dwarf Luminosity Function. *ApJ*, 352:605, April 1990. doi: 10.1086/168562.

[65] Shuji Ogata, Hiroshi Iyetomi, Setsuo Ichimaru, and Hugh M. van Horn. Equations of state and phase diagrams for dense multi-ionic mixture plasmas. *Phys. Rev. E*, 48(2):1344–1358, August 1993. doi: 10.1103/PhysRevE.48.1344.

[66] T. D. Oswalt, J. A. Smith, M. A. Wood, and P. Hintzen. A lower limit of 9.5 Gyr on the age of the Galactic disk from the oldest white dwarf stars. *Nature*, 382:692–694, August 1996. doi: 10.1038/382692a0.

[67] Adriano Pietrinferni, Santi Cassisi, Maurizio Salaris, and Fiorella Castelli. A Large Stellar Evolution Database for Population Synthesis Studies. I. Scaled Solar Models and Isochrones. *ApJ*, 612(1):168–190, September 2004. doi: 10.1086/422498.

[68] A. Y. Potekhin and G. Chabrier. Thermodynamic Functions of Dense Plasmas: Analytic Approximations for Astrophysical Applications. *Contributions to Plasma Physics*, 50(1): 82–87, January 2010. doi: 10.1002/ctpp.201010017.

[69] Pier Giorgio Prada Moroni and Oscar Straniero. Calibration of White Dwarf Cooling Sequences: Theoretical Uncertainty. *ApJ*, 581(1):585–597, December 2002. doi: 10.1086/344052.

[70] A. Rebassa-Mansergas, S. Toonen, S. Torres, and P. Canals. The effects of unresolved double degenerates in the white dwarf luminosity function. *MNRAS*, 491(4):5671–5681, February 2020. doi: 10.1093/mnras/stz3371.

[71] I. Renedo, L. G. Althaus, M. M. Miller Bertolami, A. D. Romero, A. H. Córsico, R. D. Rohrmann, and E. García-Berro. New Cooling Sequences for Old White Dwarfs. *ApJ*, 717 (1):183–195, July 2010. doi: 10.1088/0004-637X/717/1/183.

[72] Harvey B. Richer, Ilaria Caiazzo, Helen Du, Steffani Grondin, James Hegarty, Jeremy Heyl, Ronan Kerr, David R. Miller, and Sarah Thiele. Massive White Dwarfs in Young Star Clusters. *ApJ*, 912(2):165, May 2021. doi: 10.3847/1538-4357/abdeb7.

[73] A. D. Romero, F. Campos, and S. O. Kepler. The age-metallicity dependence for white dwarf stars. *MNRAS*, 450(4):3708–3723, July 2015. doi: 10.1093/mnras/stv848.

[74] Alejandra D. Romero, A. H. Córsico, B. G. Castanheira, F. C. De Gerónimo, S. O. Kepler, D. Koester, A. Kawka, L. G. Althaus, J. J. Hermes, C. Bonato, and A. Gianninas. Probing the Structure of Kepler ZZ Ceti Stars with Full Evolutionary Models-based Asteroseismology. *ApJ*, 851(1):60, December 2017. doi: 10.3847/1538-4357/aa9899.

[75] N. Rowell and N. C. Hambly. White dwarfs in the SuperCOSMOS Sky Survey: the thin disc, thick disc and spheroid luminosity functions. *MNRAS*, 417:93–113, October 2011. doi: 10.1111/j.1365-2966.2011.18976.x.

[76] M. Salaris, S. Cassisi, A. Pietrinferni, P. M. Kowalski, and J. Isern. A Large Stellar Evolution Database for Population Synthesis Studies. VI. White Dwarf Cooling Sequences. *ApJ*, 716 (2):1241–1251, June 2010. doi: 10.1088/0004-637X/716/2/1241.

[77] M. Salaris, L. G. Althaus, and E. García-Berro. Comparison of theoretical white dwarf cooling timescales. *A&A*, 555:A96, July 2013. doi: 10.1051/0004-6361/201220622.

[78] Maurizio Salaris and Santi Cassisi. Chemical element transport in stellar evolution models. *Royal Society Open Science*, 4(8):170192, August 2017. doi: 10.1098/rsos.170192.

[79] Maurizio Salaris, Inmaculada Domínguez, Enrique García-Berro, Margarida Hernanz, Jordi Isern, and Robert Mochkovitch. The Cooling of CO White Dwarfs: Influence of the Internal Chemical Distribution. *ApJ*, 486(1):413–419, September 1997. doi: 10.1086/304483.

[80] Maurizio Salaris, Aldo Serenelli, Achim Weiss, and Marcelo Miller Bertolami. Semi-empirical White Dwarf Initial-Final Mass Relationships: A Thorough Analysis of Systematic Uncertainties Due to Stellar Evolution Models. *ApJ*, 692(2):1013–1032, February 2009. doi: 10.1088/0004-637X/692/2/1013.

[81] Maurizio Salaris, Santi Cassisi, Adriano Pietrinferni, and Sebastian Hidalgo. The updated BASTI stellar evolution models and isochrones - III. White dwarfs. *MNRAS*, 509(4):5197–5208, February 2022. doi: 10.1093/mnras/stab3359.

[82] Didier Saumon, Simon Blouin, and Pier-Emmanuel Tremblay. Current challenges in the physics of white dwarf stars. *Phys. Rep.*, 988:1–63, November 2022. doi: 10.1016/j.physrep.2022.09.001.

[83] E. Schatzman. Solidification of carbon-oxygen white dwarfs. In *2d International Colloquium on Drops and Bubbles*, pages 222–226, March 1982.

[84] E. L. Schatzman. *White dwarfs*. 1958.

[85] Josiah Schwab. Evolutionary Models for the Remnant of the Merger of Two Carbon-Oxygen Core White Dwarfs. *ApJ*, 906(1):53, January 2021. doi: 10.3847/1538-4357/abc87e.

[86] L. Segretain. Three-body crystallization diagrams and the cooling of white dwarfs. *A&A*, 310:485–488, June 1996.

[87] L. Segretain, G. Chabrier, M. Hernanz, E. Garcia-Berro, J. Isern, and R. Mochkovitch. Cooling theory of crystallized white dwarfs. *ApJ*, 434:641–651, October 1994. doi: 10.1086/174766.

[88] G. Shaviv and A. Kovetz. The cooling of carbon-oxygen white dwarfs. *A&A*, 51(3):383–391, September 1976.

[89] Ken J. Shen, Simon Blouin, and Katelyn Breivik. The Q Branch Cooling Anomaly Can Be Explained by Mergers of White Dwarfs and Subgiant Stars. *ApJ*, 955(2):L33, October 2023. doi: 10.3847/2041-8213/acf57b.

[90] David R. Soderblom. The Ages of Stars. *ARA&A*, 48:581–629, September 2010. doi: 10.1146/annurev-astro-081309-130806.

[91] D. J. Stevenson. A eutectic in carbon-oxygen white dwarfs? *Journal de Physique*, 41:C2 61–C2 64, March 1980.

[92] M. Tassoul, G. Fontaine, and D. E. Winget. Evolutionary Models for Pulsation Studies of White Dwarfs. *ApJS*, 72:335, February 1990. doi: 10.1086/191420.

[93] Jordi Tononi, Santiago Torres, Enrique García-Berro, María E. Camisassa, Leandro G. Althaus, and Alberto Rebassa-Mansergas. Effects of ^{22}Ne sedimentation and metallicity on the local 40 pc white dwarf luminosity function. *A&A*, 628:A52, August 2019. doi: 10.1051/0004-6361/201834267.

[94] P.-E. Tremblay, G. Fontaine, N. P. G. Fusillo, B. H. Dunlap, B. T. Gänsicke, M. A. Hollands, J. J. Hermes, T. R. Marsh, E. Cukanovaite, and T. Cunningham. Core crystallization and pile-up in the cooling sequence of evolving white dwarfs. *Nature*, 565:202–205, January 2019. doi: 10.1038/s41586-018-0791-x.

[95] B. A. Twarog. The chemical evolution of the solar neighborhood. II - The age-metallicity relation and the history of star formation in the galactic disk. *ApJ*, 242:242–259, November 1980. doi: 10.1086/158460.

[96] H. M. van Horn. Crystallization of White Dwarfs. *ApJ*, 151:227, January 1968. doi: 10.1086/149432.

[97] V. Weidemann. Mass loss towards the white dwarf stage. *A&A*, 59(3):411–418, August 1977.

[98] V. Weidemann. The initial-final mass relation : galactic disk and Magellanic Clouds. *A&A*, 188:74–84, December 1987.

[99] V. Weidemann. Revision of the initial-to-final mass relation. *A&A*, 363:647–656, November 2000.

[100] Volker Weidemann. White Dwarfs. *ARA&A*, 6:351, January 1968. doi: 10.1146/annurev.aa.06.090168.002031.

[101] S. P. Wyatt and J. H. Cahn. Kinematics and ages of Mira variables in the greater solar neighborhood. *ApJ*, 275:225–239, December 1983. doi: 10.1086/161527.

[102] Z. W. Xu and H. M. van Horn. Effects of Fe/C Phase Separation on the Ages of White Dwarfs. *ApJ*, 387:662, March 1992. doi: 10.1086/171115.